





Article

Cd(II) and Pd(II) Mixed Ligand Complexes of Dithiocarbamate and Tertiary Phosphine Ligands—Spectroscopic, Anti-Microbial, and Computational Studies

Tohama B. Abdullah ¹, Reza Behjatmanesh-Ardakani ², Ahmed S. Faihan ¹ , Hayfa M. Jirjes ¹,
Mortaga M. Abou-Krishna ^{3,4} , Tarek A. Yousef ^{3,5} , Sayed H. Kenawy ^{3,6} and Ahmed S. M. Al-Janabi ^{1,*} 

¹ Department of Chemistry, College of Science, University of Tikrit, Tikrit 34001, Iraq

² Department of Chemistry, Payame Noor University, Tehran 19395-4697, Iran

³ Chemistry Department, Science College, Imam Mohammad Ibn Saud Islamic University, Riyadh 11623, Saudi Arabia

⁴ Department of Chemistry, South Valley University, Qena 83523, Egypt

⁵ Mansoura Laboratory, Toxic and Narcotic Drug, Forensic Medicine Department, Medicolegal Organization, Ministry of Justice, Cairo 11435, Egypt

⁶ Ceramics and Building Materials Department, National Research Centre, Refractories, El-Buhouth St., Dokki, Giza 12622, Egypt

* Correspondence: dr.ahmed.chem@tu.edu.iq

Abstract: Mixed ligand complexes of Pd(II) and Cd(II) with *N*-picolyl-amine dithiocarbamate (PAC-dtc) as primary ligand and tertiary phosphine ligand as secondary ligands have been synthesized and characterized via elemental analysis, molar conductance, NMR (¹H and ³¹P), and IR techniques. The PAC-dtc ligand displayed in a monodentate fashion via sulfur atom whereas diphosphine ligands coordinated as a bidentate mode to afford a square planar around the Pd(II) ion or tetrahedral around the Cd(II) ion. Except for complexes [Cd(PAC-dtc)₂(dppe)] and [Cd(PAC-dtc)₂(PPh₃)₂], the prepared complexes showed significant antimicrobial activity when evaluated against *Staphylococcus aureus*, *Pseudomonas aeruginosa*, *Candida albicans* and *Aspergillus niger*. Moreover, DFT calculations were performed to investigate three complexes {[Pd(PAC-dtc)₂(dppe)](1), [Cd(PAC-dtc)₂(dppe)](2), [Cd(PAC-dtc)₂(PPh₃)₂](7)}, and their quantum parameters were evaluated using the Gaussian 09 program at the B3LYP/LanL2dz theoretical level. The optimized structures of the three complexes were square planar and tetrahedral geometry. The calculated bond lengths and bond angles showed a slightly distorted tetrahedral geometry for [Cd(PAC-dtc)₂(dppe)](2) compared to [Cd(PAC-dtc)₂(PPh₃)₂](7) due to the ring constrain in the dppe ligand. Moreover, the [Pd(PAC-dtc)₂(dppe)](1) complex showed higher stability compared to Cd(2) and Cd(7) complexes which can be attributed to the higher back-donation of Pd(1) complex.

Keywords: picolylamine; dithiocarbamate; single-pot reaction; DFT; complexes



Citation: Abdullah, T.B.; Behjatmanesh-Ardakani, R.; Faihan, A.S.; Jirjes, H.M.; Abou-Krishna, M.M.; Yousef, T.A.; Kenawy, S.H.; Al-Janabi, A.S.M. Cd(II) and Pd(II) Mixed Ligand Complexes of Dithiocarbamate and Tertiary Phosphine Ligands—Spectroscopic, Anti-Microbial, and Computational Studies. *Molecules* **2023**, *28*, 2305. <https://doi.org/10.3390/molecules28052305>

Academic Editor: Alistair J. Lees

Received: 27 January 2023

Revised: 16 February 2023

Accepted: 23 February 2023

Published: 2 March 2023



Copyright: © 2023 by the authors. Licensee MDPI, Basel, Switzerland. This article is an open access article distributed under the terms and conditions of the Creative Commons Attribution (CC BY) license (<https://creativecommons.org/licenses/by/4.0/>).

1. Introduction

Growing interest in ligands bearing N and S donor atoms have attracted a lot of attention due to their interesting structural and biological properties [1–8]. Dithiocarbamate, a unique dithiolate ligand, has been increasingly reported in the literature because of its strong chelating capability [2]. This behavior can be explained in terms of its stable resonance structures (Figure 1).

The resulting delocalized pi-electrons through the N-CS₂ group can provide additional stability (Figure 2).

In addition, the d π vacant orbital on the S atom can serve as a multi donor atom with multiple pi-bonds [9]. Despite the vast literature coverage of dithiocarbamate metal complexes, interest has only been directed at the secondary amine dithiocarbamate. Primary amine dithiocarbamate on the other hand, has been poorly represented in the literature [10].

The acidic proton accompanied with its low stability could be the reason primary amines are not a good candidate for dithiocarbamate synthesis [10]. Cadmium dithiocarbamate complexes have received little attention and only a few examples have been shown in the literature [11–13]. The majority of the reported complexes showed dimer characteristics. Cadmium with a dithiocarbamate moiety has also been shown to coordinate with donor atoms of sulfur, nitrogen, and phosphorus [14]. However, the dithiocarbamate ligands and their complexes have drawn considerable interest because of their intriguing biological characteristics [15–17]. Moreover, they have applications in areas as diverse as medicine, agriculture, biological imaging, and materials science; they are extremely versatile ligands, forming stable complexes with all the transition metals, along with the lanthanides, the actinides, and a majority of the p-block elements. At the same time, their ability to adopt resonance hybrids allows for stabilizing metals in both high and low oxidation states [16–26]. Over the past decade, the development of dithiocarbamate chemistry has continued unabated with applications in areas including novel inorganic drugs, capping agents for nano-engineered surfaces and other nanomaterials, including quantum dots, and the rational construction of well-defined complex molecular structures [17–26].

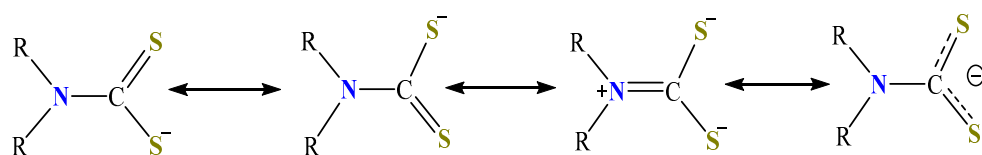


Figure 1. Dithiocarbamate resonance structures.

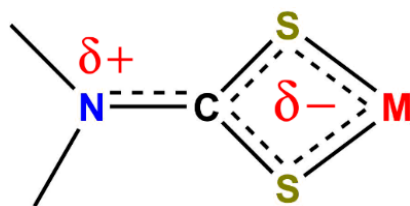


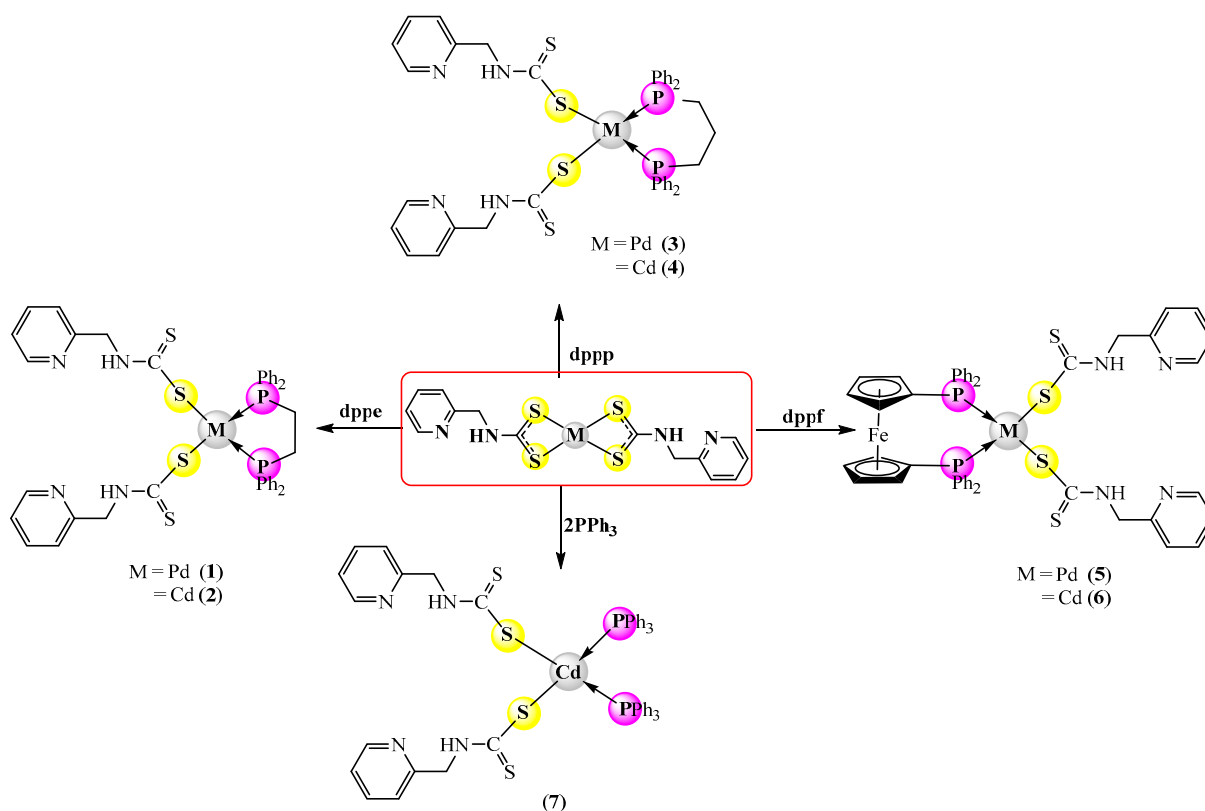
Figure 2. π -electrons delocalization through N-CS₂ group.

In the current efforts to develop the coordination chemistry of primary amine dithiocarbamate complexes, including phosphine ligands, we used the *N*-picolyl-amine dithiocarbamate metal complex (MII = Cd, Pd) as a base for the synthesis of some mixed ligand complexes containing tertiary phosphine ligands.

2. Results

2.1. Synthesis

The heteroleptic Pd(II) and Cd(II) complexes were synthesized by treating [Pd(PCA-dtc)₂] and [Cd(PCA-dtc)₂] with equivalent molar diphosphine (dppe, dppp, dppf) or with two equivalents of triphenyl phosphine (PPh₃) under reflux conditions in chloroform (Scheme 1). They are stable in air, and their solubility was found in DMSO and DMF and was analyzed by elemental analysis, molar conductivity and spectroscopic techniques (¹H, ¹³C NMR, mass, IR, and UV-visible). The molar conductivity of the complexes in DMSO revealed that they were neutral as expected [27]. The results indicated that PAC-dtc ligands were bonded as a monodentate fashion through the sulfur atom, whereas the diphosphine ligands (dppe, dppp and dppf) bonded as bidentate chelating, while triphenyl phosphine was coordinated as monodentate model. The geometry around Pd(II) ion is a square plane, but a tetrahedral around Cd(II) ion.



Scheme 1. Synthesis of complexes (1–7).

2.2. Characterization of Prepared Complexes

Characterization was relatively natural on the fundamental of spectral and analytical data (Tables 1–3).

Table 1. Physical properties and elemental analysis.

Seq.	Color	Yield (%)	Conductivity	m.p (°C)	Elemental Analysis		
					Calc. (Found) %		
					C	H	N
1	Greenish yellow	91	12.1	190–192	55.14 (54.93)	4.40 (4.61)	6.43 (6.78)
2	White	74	8.0	162–165	54.76 (54.90)	4.37 (4.20)	6.39 (6.45)
3	Greenish yellow	89	3.8	152–154	55.62 (55.78)	4.55 (4.72)	6.33 (6.51)
4	Olive	86	2.9	89–92	55.24 (55.37)	4.52 (4.43)	6.29 (6.48)
5	Dark brown	92	10.1	168–174	56.12 (56.06)	4.12 (3.98)	5.45 (5.71)
6	Olive	45	11.0	121–124	55.79 (55.81)	4.10 (3.96)	5.42 (5.70)
7	Green	96	13.8	101–103	59.84 (59.74)	4.42 (4.71)	5.58 (5.62)

Table 2. ^{31}P and ^1H nmr chemical shifts of the synthesized complexes.

Complexes	δP (ppm)	δH (ppm)			
		NH	CH_2 or H-Cp PAC-dtc	CH_2 phosphine	Aryl Rings
1	30.60	11.58 (<i>s</i> , 2H)	4.93 (<i>s</i> , 4H)	2.43 (<i>s</i> , 4H)	7.49–8.84 (<i>m</i> , 28H)
2	30.34	13.37 (<i>bs</i> , 2H)	4.40 (<i>s</i> , 4H)	2.72 (<i>s</i> , 4H)	6.63–8.11 (<i>m</i> , 28H)
3	30.23	10.28 (<i>s</i> , 2H)	4.32 (<i>s</i> , 2H)	3.01 (<i>bs</i> , 4H); 1.89 (<i>bs</i> , 2H);	6.97–8.11 (<i>m</i> , 28H)
4	30.28	11.04 (<i>bs</i> , 2H)	4.46 (<i>s</i> , 2H)	3.09 (<i>s</i> , 4H); 1.84 (<i>s</i> , 2H);	6.81–8.39 (<i>m</i> , 28H)
5	26.00	10.71 (<i>s</i> , 2H)	4.35 (<i>s</i> , 4H)	4.84 (<i>bs</i> , 8H)	6.96–8.85 (<i>m</i> , 28H)
6	39.83	10.84 (<i>d</i> , 2H)	4.21 (<i>d</i> , 4H)	4.90–5.28 (<i>m</i> , 8H)	6.70–8.66 (<i>m</i> , 28H)
7	25.83	10.45 (<i>d</i> , 2H)	4.25 (<i>dd</i> , 4H)	–	6.64–8.68 (<i>m</i> , 38H)

Table 3. IR data of the synthesized complexes in (cm^{-1}).

Comps.	$\nu(\text{N-H})$	$\nu(\text{C-H})$		Phosphine Ligands			$\nu(\text{C=N})_{\text{pyridyl}}$ $\nu(\text{C-N})$	$\nu(\text{CS}_2)$	$\nu(\text{M-P})$ $\nu(\text{M-S})$
		Aliph.	Arom.	$\nu(\text{P-Ph})$	$\nu(\text{P-C})_{\text{st}}$	$\delta(\text{P-C})$			
1	3203b	3057w	2943w	1435s	1119s	532s	1618m 1533s	1001m 694s	493w 428w
2	3331m	3008w	2918w	1433s	1093s	530s	1595m 1533s	987m 694s	479w 425w
3	3308b	3108w	2943w	1433s	1120s	511s	1624m 1533s	1001m 694s	463w 424w
4	3338m	3053w	2935w	1437s	1118s	509s	1618m 1541s	995m 694s	464w 427w
5	3318m	3103w	2947w	1433s	1118s	532s	1622s 1531s	1001m 698s	491w 440w
6	3291m	3057w	2953w	1437s	1120s	497s	1623m 1541s	1036m 700m	497w 424w
7	3318m	3053w	2947w	1437s	1120s	502s	1595s 1548s	997m 694m	462w 412w

2.2.1. $^{31}\text{P}\{-^1\text{H}\}$ and ^1H nmr Spectra

The $^{31}\text{P}\{-^1\text{H}\}$ nmr spectra of the complexes (1–7) showed a singlet peak for each at δ 30.42 ppm, δ 37.19, δ 30.42 ppm, δ 37.19, δ 30.42 ppm, δ 37.19 ppm, and δ 30.22 ppm, respectively (Figures S1–S7) and (Table 2), indicating the appearance of a single isomer for each and the phosphorus atoms are equivalents; we propose that this isomer is maybe the S-bonded one.

In the ^1H NMR spectra of complexes (1) and (2) (Figures S8 and S9), they displayed a singlet peak at δH 2.43 and 2.72 ppm for CH_2 of dppe ligand, respectively. Whereas the CH_2 of PAC-dtc ligand was displayed at δH 4.93 and 4.40 ppm, respectively. In addition, the spectra showed the proton of the NH group at δH 11.58 and 13.37 ppm, respectively. Finally, the phenyl protons of the diphosphine and PAC-dtc ligands appeared as unresolved multiplets within the δ 6.63–8.84 ppm range. Integration of the signals agreed well with the formula. The ^1H NMR spectra of complexes (3) and (4) (Figures S10 and S11), displayed two broad singlets at δH (3.01, 3.09) ppm and δH (1.89, 1.84) ppm corresponding to the two different methylene groups for the phosphine ligand. The protons for the CH_2 and NH groups of PAC-dtc ligand appeared as two separated peaks at δH (4.32, 4.46) and δ (10.28, 11.03), respectively. The phenyl protons of the phosphine and PAC-dtc ligands appeared as multiplets within the δH 6.81–8.39 ppm range.

In ^1H NMR spectra of complexes (5) and (6) (Figures S12 and S13), the CH_2 and NH groups of **PAC-dtc** ligand appeared as two separate peaks at δH (4.21, 4.35) ppm and δH (10.71, 10.84) ppm, respectively, whereas the protons of the cyclopentadiene of **dppf** ligand appeared at δH 4.84 ppm, for the two complexes, respectively. The phenyl protons showed as unresolved multiplet peaks within the δH 6.70–8.85 ppm range. The ^1H NMR spectrum of $[\text{Cd}(\text{PCA-dtc})_2(\text{PPh}_3)_2]$ (7) (Figure S14), showed two peaks at δH 4.25 and 10.45 ppm due to the CH_2 and NH groups for the **PAC-dtc** ligand, respectively. The phenyl protons were showed as unresolved multiplets peak within the δH 6.64–8.68 ppm range.

2.2.2. IR Data

The IR data of the synthesized complexes were assigned and are presented in Table 3. Three new bands displayed in the IR spectra of the $[\text{M}(\text{PAC-dtc})_2(\text{diphos})]$ ($\text{M}^{\text{II}} = \text{Pd}$ and Cd) complexes which were not found in the spectra of $[\text{M}(\text{PAC-dtc})_2]$ complexes, within $(1433\text{--}1437)\text{ cm}^{-1}$, $(1093\text{--}1120)\text{ cm}^{-1}$ and $(497\text{--}532)\text{ cm}^{-1}$ range, due to the $\nu(\text{P-Ph})$, $\nu(\text{P-C})_{\text{stretching}}$, and bending of (P-C) band, respectively [28–34]. It is thought [34] that this vibration arises from the deformation of the planarity of the phenyl ring bonded to a heavy atom (phosphorus).

The CS_2 thiocarbonyl stretching splits into two peaks (double and single) with medium intensity within $(694\text{--}700)\text{ cm}^{-1}$ and $(1036\text{--}987)\text{ cm}^{-1}$ range for complexes (1–7) [35,36]. The spectroscopic data suggest that the **PAC-dtc** ligand coordinated in a monodentate fashion through the sulfur atom with $\text{Pd}(\text{II})$ and $\text{Cd}(\text{II})$ ions. In addition, the IR spectra displayed the NH vibrations within the $(3291\text{--}3338)\text{ cm}^{-1}$ range. Whereas the frequencies $\text{C}=\text{N}$ of pyridyl ring and $\text{C}-\text{N}$ aliphatic appeared within $(1595\text{--}1624)\text{ cm}^{-1}$ and $(1531\text{--}1548)\text{ cm}^{-1}$. Two other new characteristic bands appeared within $(412\text{--}440)\text{ cm}^{-1}$ and $(462\text{--}497)\text{ cm}^{-1}$ assigned to the $\nu(\text{M-S})$ [36–38] and $\nu(\text{M-P})$ [36,37], respectively.

2.3. Antimicrobial Studies

Seven mixed ligand complexes (1–7) were screened for their antibacterial activity against *Staphylococcus aureus* and *Pseudomonas aeruginosa* using the cup-plate method [33]. Additionally, the antifungal ability of these complexes was tested against two fungal species *Candida albicans* and *Aspergillus niger* using the disc diffusion method [39]. The standard error for the experiment was $\pm 0.03\%$, and the experiments were repeated three times in the same conditions.

The antibacterial activity results against the tested bacteria revealed that most of the compounds have shown moderate to excellent activity. Complexes 5 and 6 displayed good antibacterial activity against pathogenic bacteria species in comparison with the standard Gentamicin and other prepared compounds, which may be due to the presence of iron element in the structure of diphosphine ligand (**dppf**) in addition to the electron-donating atoms (N and S) of pyridyl and dithiocarbamate groups. The antibacterial activity order is as follows:

$$5 > 6 > 1 > 4 > 3 > 2 > 7$$

In similar antifungal results, it is evident that Complexes 5 and 6 displayed good to excellent restraint effects against *Candida albicans* and *Aspergillus niger* compared to Fluconazole. It may be due to the presence of iron element in the structure of **dppf** ligand with electron-donating atoms (N and S) of pyridyl and dithiocarbamate groups; the results of these antimicrobial activities are listed in Table S1.

2.4. Computational Studies

2.4.1. Geometrical and Electronic Properties

The optimized structures of complexes (**Pd(1)**, **Cd(2)**, **Cd(7)**) are shown in (Figure 3). These complexes all have a (+2) central ion due to the hydrogen loss of SH in each S-containing ligand. Two structures—square planar and tetrahedral geometry—have been found in the geometry of the complexes under study. $\text{Pd}(\text{II})$ in the **Pd(1)** complex, for instance, has square planar geometry, but $\text{Cd}(\text{II})$ in the **Cd(2)** and **Cd(7)** complexes has

tetrahedral geometry. The calculated bond angles have shown different values for each complex. For instance, Cd(2) and Cd(7) have substantially different angles between Cd(II) and the donor atoms. The bond angle of P–Cd–P in Cd(2) is 79.5° , while it is 109.2° in Cd(7). In addition, the S–Cd–S angle in Cd(2) and Cd(7) is 122.5° and 120.9° , respectively. These results demonstrate that the distortion in Cd(2) is greater than the distortion in Cd(7). Tetrahedral symmetry in its optimal form has an angle of 109.5° . However, the angles in the Cd(2) and Cd(7) complexes are not perfect. Pd(1) complex on the other hand, showed a distorted square planar geometry. The calculated bond angles are $100, 86, 87$ and 87° , which are normal for square planar configuration. Similarly, the bond lengths values of the complexes under study have also shown some variations. These differences arise from the fact that the dppe ligand has generated a constraint on the overall complex structure which affects both the bond distances and the bond angles. For instance, the Cd–S bond lengths of Cd(2) are 2.50 and 2.52 Å, while in Cd(7) complex these are 2.52 and 2.54 Å. The Cd–P bond lengths in Cd(2) complex are 2.74 and 2.77 Å, whereas in Cd(7) complex these are 2.77 and 2.84 Å.

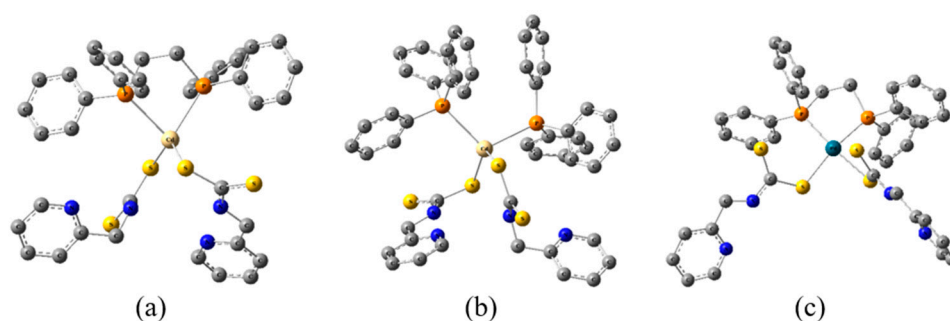


Figure 3. Optimized structures for (a) Cd(2), (b) Cd(7) and (c) Pd(1); hydrogen atoms were not shown for simplicity.

The highest occupied molecular orbital (HOMO) and the lowest unoccupied molecular orbital (LUMO) are calculated at the level of B3LYP/Def2-TZVP (Figure 4). The HOMO–LUMO energy gap for Pd(1) is less than the two other complexes. These findings imply that Pd(1) is a good candidate for a photo catalyst material that activates electron-hole pairs in the solar energy zone. According to Figure 4, HOMO are primarily localized on ligands that contain S, while LUMO are primarily localized on ligands that contain P. This is consistent with the estimated charges on the atoms of P and S. (see Table 4). The electronegativity of P atoms is lower than that of S and N atoms. In contrast to their role in LUMO, the P atoms do not contribute to HOMO charge density.

Table 4. NBO charges for the central ion and the connected atoms.

Complex	S	S	P	P	Cd/Pd
Cd(2)	−0.46	−0.41	+0.73	+0.73	+1.27
Cd(7)	−0.47	−0.42	+0.78	+0.78	+1.26
Pd(1)	−0.17	−0.15	+1.0	+1.0	+0.26

2.4.2. NBO Analysis

In Table 5, the natural bond orbital (NBO) charges for selected atoms in the complexes under study have been listed. The core metal ions' charges in each of the three complexes shift from +2 to a less positive value. These outcomes show a charge transfer from ligand to metal. The NBO charge for Cd changes from +2 to +1.26, while the NBO charge for Pd changes from +2 to +0.26. This shows that there is a higher ligand to metal charge transfer (LMCT) for Pd compared to Cd. The NBO charges on S atoms are negative, but less than one, which indicates that these atoms donate their valence charge to the Cd(II)/Pd(II) atoms. The results demonstrate that S atom in Pd(1) complex has a lower negative charge than S atoms in Cd(2) and Cd(7) complexes, indicating a stronger electron donation to Pd

(II). However, compared to two other complexes, the NBO charge on the P atom in the **Pd(1)** complex is greater positive. As a result, the **Pd(1)** complex had a stronger charge donation from ligand to metal than the **Cd(2)** and **Cd(7)** complexes.

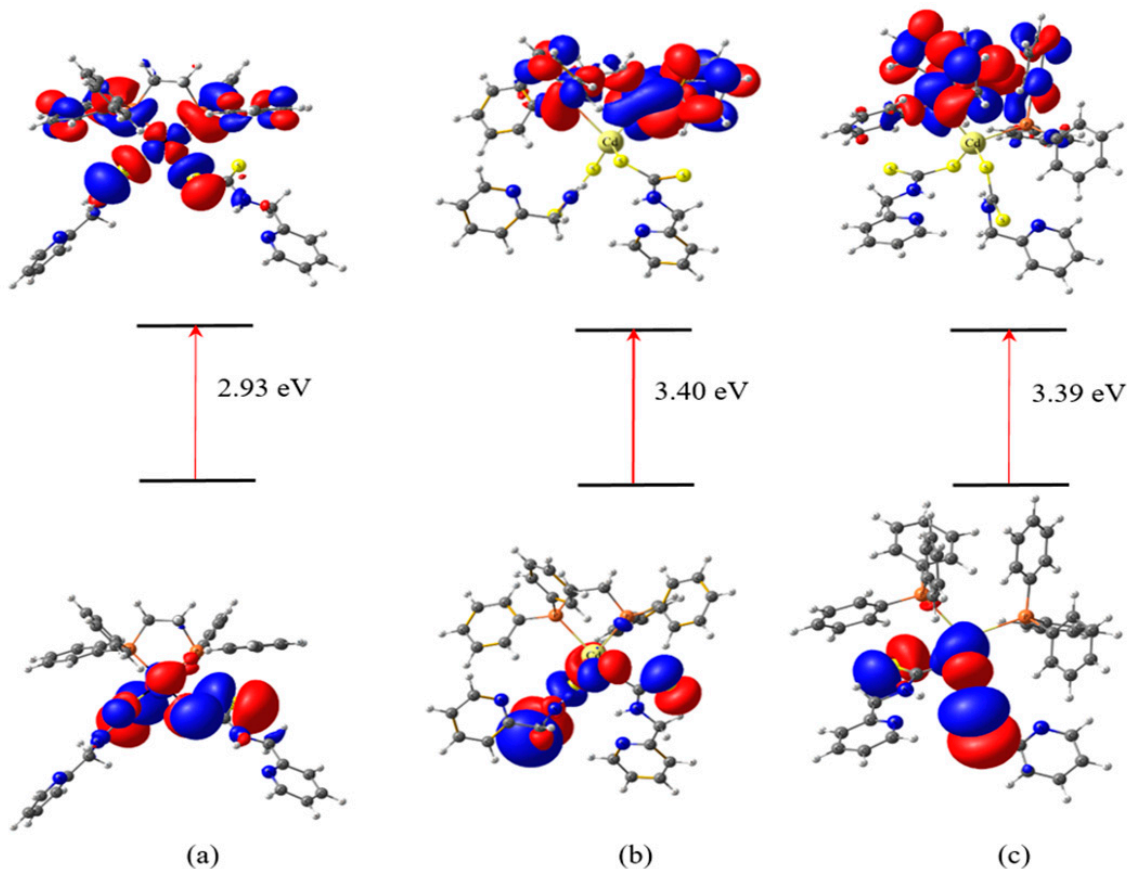


Figure 4. HOMO and LUMO for (a) **Pd(1)**, (b) **Cd(2)** and (c) **Cd(7)**.

Table 5. Second order perturbation energies for charge transfers from donor to acceptor orbitals in **Pd(1)**.

Donor	Type	Acceptor	Type	$E^{(2)}$
(LP1) _{P28}	13% (s) + 87% (p)	P12-Pd53	σ^*	71.5
(LP1) _{P28}	13% (s) + 87% (p)	C25-P28	σ^*	23.6
(LP1) _{P28}	13% (s) + 87% (p)	P28-C31	σ^*	22.0
(LP1) _{P28}	13% (s) + 87% (p)	P28-C42	σ^*	23.8
(LP1) _{P28}	13% (s) + 87% (p)	Pd53-S54	σ^*	236.5
(LP2) _{S54}	100% (p)	C56-S72	π^*	47.0
(LP1) _{N58}	100% (p)	C56-S72	π^*	81.5
(LP2) _{S72}	100% (p)	C56-N58	σ^*	12.1
P12-Pd53	σ	Pd53-S54	σ^*	31.5
Pd53-S54	σ	P12-Pd53	σ^*	66.7
Pd53-S54	σ	Pd53-S54	σ^*	21.5
(LP2) _{S55}	74% (s) + 26% (p)	P12-Pd53	σ^*	12.3
(LP3) _{S55}	100% (p)	P12-Pd53	σ^*	106.5
(LP3) _{S55}	100% (p)	Pd53-S54	σ^*	19.4
(LP2) _{S55}	100% (p)	C57-S87	σ^*	43.9
(LP1) _{N73}	100% (p)	C57-S87	σ^*	85.2
(LP2) _{S87}	100% (p)	C57-N73	σ^*	12.5

Second order perturbation energy ($E^{(2)}$) was calculated to investigate how much these charge transfers stabilize the complexes. Tables 5–7 show the results of the second order

perturbation energies due to the charge transfer from donor orbitals to the acceptor ones. Figures 5 and 6 graphically represent donor and acceptor orbitals for the two highest second order perturbation energies. In line with the previous discussion, P and S atoms are very good electron donors to the central metal ions. The maximum $E^{(2)}$ for **Cd(2)** and **Cd(7)** complexes belong to S donors, while the highest $E^{(2)}$ for **Pd(1)** complex belong to P donors. P orbitals (in hybridized or pure forms) are the main type of donor orbitals in all three complexes. N is a lot less active donor in these complexes compared to our earlier study [16]. Additionally, unlike the Pt complexes examined earlier [37], there is no back-donation charge transfer in these complexes. Based on the obtained data, the 6s orbital in **Cd(2)** and **Cd(7)** complexes is the best electron acceptor. According to NBO analysis, **Pd(1)** complex's anti-binding orbitals of Pd-S and Pd-P are the best electron acceptors.

Table 6. Second order perturbation energies for charge transfers from donor to acceptor orbitals in **Cd(2)**.

Donor	Type	Acceptor	Type	$E^{(2)}$
(LP1) _{P1}	45% (s) + 55% (p)	(LV) _{Cd47}	100% (s)	64.0
(LP1) _{S48}	70% (s) + 30% (p)	(LV) _{Cd47}	100% (s)	7.4
(LP2) _{S48}	7% (s) + 93% (p)	(LV) _{Cd47}	100% (s)	7.9
(LP3) _{S48}	8% (s) + 92% (p)	(LV) _{Cd47}	100% (s)	131.4
(LP3) _{S48}	8% (s) + 92% (p)	C50-S69	π^*	22.7
(LP1) _{N68}	100% (p)	C50-S69	π^*	70.8
(LP2) _{S48}	7% (s) + 93% (p)	N52-H67	σ^*	8.3
(LP3) _{S49}	12% (s) + 88% (p)	(LV) _{Cd47}	100% (s)	140.0
(LP2) _{S49}	100% (p)	C51-S53	σ^*	13.0
(LP1) _{N52}	100% (p)	C51-S53	σ^*	24.7
(LP1) _{N52}	100% (p)	C51-S53	π^*	14.8
(LP2) _{S53}	100% (p)	S49-C51	σ^*	10.5
(LP2) _{S53}	100% (p)	C51-N52	σ^*	11.4

Table 7. Second order perturbation energies for charge transfers from donor to acceptor orbitals in **Cd(7)**.

Donor	Type	Acceptor	Type	$E^{(2)}$
(LP1) _{P7}	45% (s) + 55% (p)	(LV) _{Cd69}	100% (s)	58.8
(LP1) _{P46}	45% (s) + 55% (p)	(LV) _{Cd69}	100% (s)	70.0
(LP3) _{S70}	8% (s) + 92% (p)	(LV) _{Cd69}	100% (s)	124.3
(LP3) _{S70}	8% (s) + 92% (p)	C72-S91	π^*	23.5
(LP1) _{N90}	100% (s)	C72-S91	π^*	72.7
(LP2) _{S91}	1% (s) + 99% (p)	S70-C72	σ^*	11.3
(LP2) _{S91}	1% (s) + 99% (p)	C72-N90	σ^*	11.4
(LP2) _{S70}	8% (s) + 92% (p)	N74-H89	σ^*	10.1
(LP3) _{S71}	12% (s) + 88% (p)	(LV) _{Cd69}	100% (s)	128.6
(LP2) _{S71}	100% (p)	C73-S75	π^*	41.3
(LP1) _{N74}	100% (p)	C73-S75	π^*	88.5
(LP2) _{S75}	100% (p)	S71-C73	σ^*	10.4
(LP2) _{S75}	100% (p)	C73-N74	σ^*	11.2

2.4.3. MEP Analysis

From a formatted check-point file, the examined complexes' molecular electrostatic potential was estimated. To do this, total electronic density was considered for MEP calculations. Different colors are used to depict the charge distribution. The red color is for negative MEP showing electron rich regions, and the blue color is for positive MEP that shows regions of electron deficiency. The highest positive and negative values of MEP were fixed to be in the range of -0.04 to $+0.04$ (Figure 7).

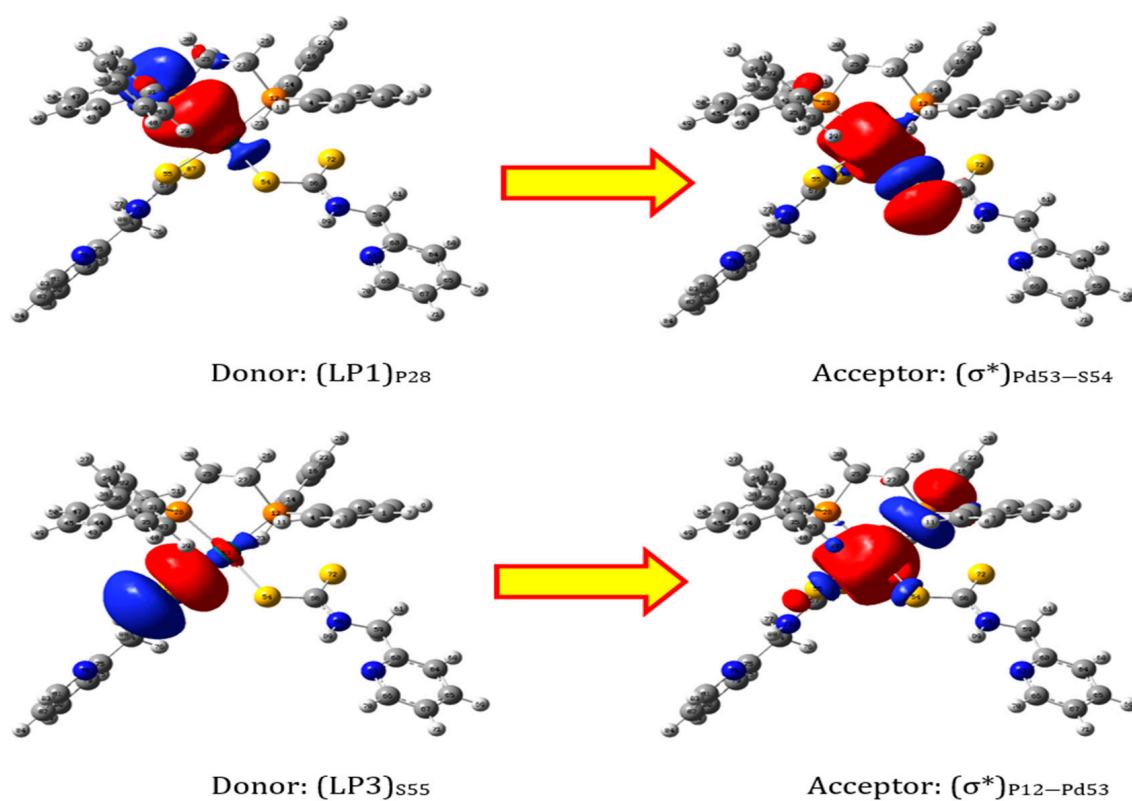


Figure 5. Donor and acceptor orbitals of two highest second order perturbation energies of Pd(1) complex.

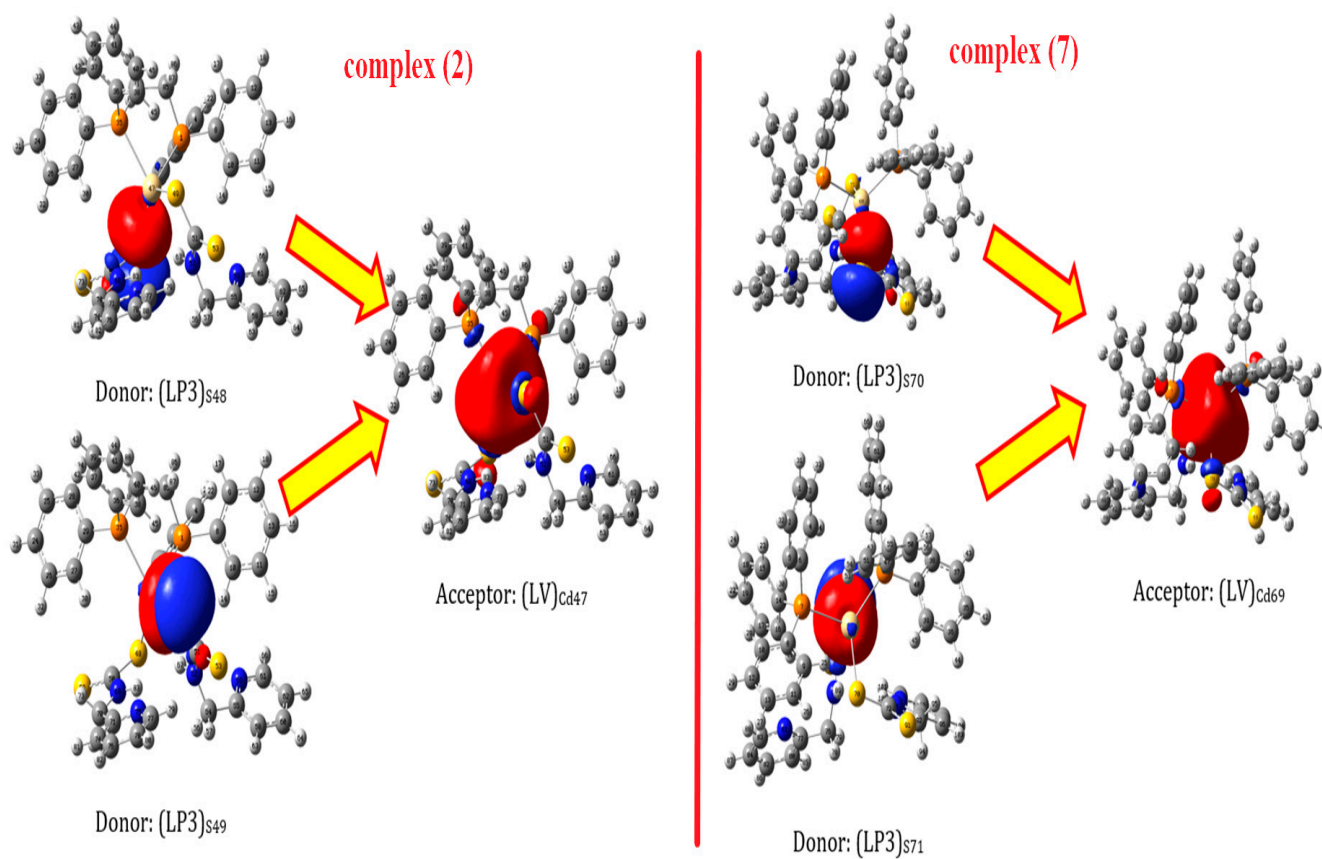


Figure 6. Two highest $E^{(2)}$ donors and acceptor orbitals for Cd(2) and Cd(7) complexes.

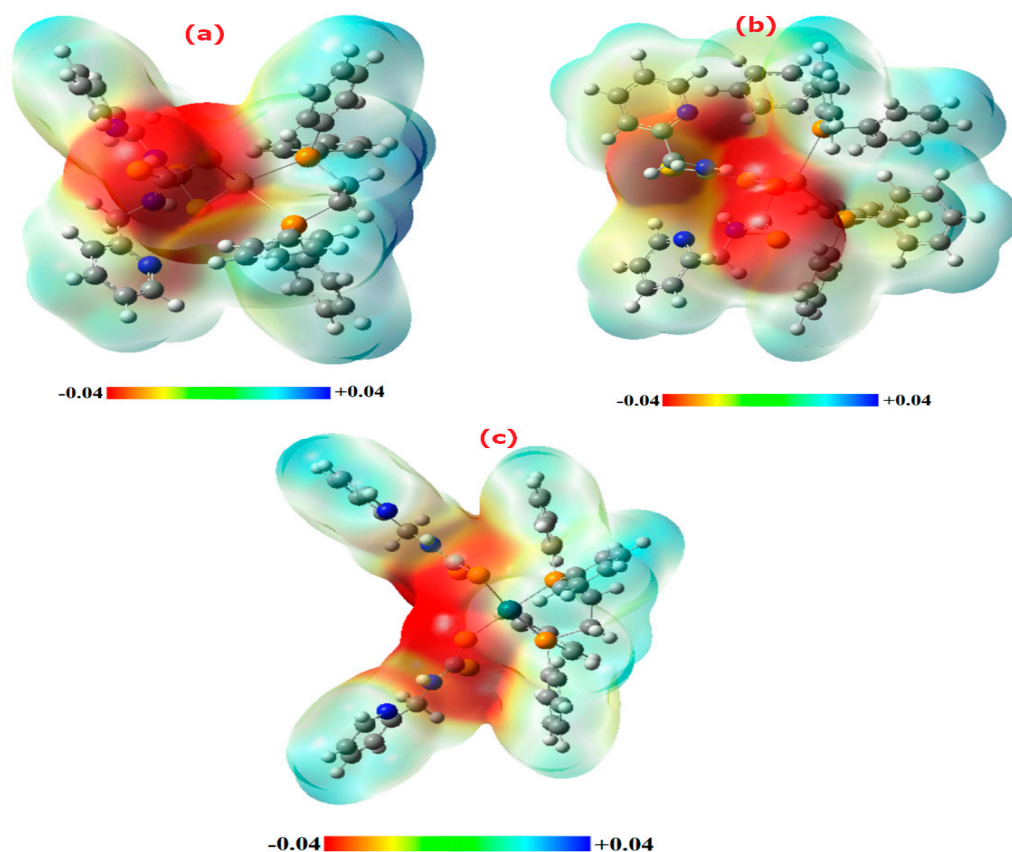


Figure 7. Molecular electrostatic potential calculated at the level of B3LYP/Def2-TZVP for (a) Cd(2) (b) Cd(2), and (c) Pd(1).

3. Experimental Part

3.1. Material and Physical Measurements

The NMR and IR spectra were recorded using an NMR-Bruker spectrophotometer (400 MHz- in DMSO- d_6 solvent) and FT-IR 8400 spectrophotometer (as KBr disc in 4000–400 cm^{-1} range). Elemental (CHN) analysis was recorded by Elementar Vario EL Cube. The molar conductivity is measured using (JENWEAY-Molar Conductivity meter) for a DMSO solution of the prepared complexes with 10^{-3} M at 25 °C. All materials used in this study were purchased from Merck or Alfa-Aser and used without further purification. The $[\text{Pd}(\text{PCA-dtc})_2]$ and $[\text{Pd}(\text{PCA-dtc})_2]$ complexes were according to the literature [40].

3.2. Synthesis of Complexes

3.2.1. Synthesis of $[\text{Pd}(\text{PCA-dtc})_2(\text{dppe})]$ Complex (1)

A solution of 1,2-bis(diphenylphosphino)ethane (dppe) (0.025 g, 0.063 mmol) in CHCl_3 (10mL) was added to a solution of a complex $[\text{Pd}(\text{PCA-dtc})_2]$ (0.030 g, 0.063 mmol) in CHCl_3 (10 mL), and a yellow suspension was formed. The mixture was refluxed for four hours. The greenish yellow mixture was left at room temperature to evaporate slowly, then a gum matter was formed, washed with ether and n-hexane several times to afford a greenish yellow ppt. then dried under vacuum. (Greenish yellow solid powder. Yield: 0.050 g, 91%. M.p (°C): 190–193).

The following complexes $[\text{Cd}(\text{PCA-dtc})_2(\text{dppe})]$ (2), $[\text{Pd}(\text{PCA-dtc})_2(\text{dppp})]$ (3), $[\text{Cd}(\text{PCA-dtc})_2(\text{dppp})]$ (4), $[\text{Pd}(\text{PCA-dtc})_2(\text{dppf})]$ (5), $[\text{Cd}(\text{PCA-dtc})_2(\text{dppf})]$ (6) were prepared and isolated in similar methods.

3.2.2. Synthesis of $[\text{Cd}(\text{PCA-dtc})_2(\text{PPh}_3)_2]$ complex (7)

A solution of triphenyl phosphine (PPh_3) (0.049 g, 0.191 mmol) in CHCl_3 (10 mL) was added to a solution of a complex $[\text{Cd}(\text{PCA-dtc})_2]$ (0.022 g, 0.045 mmol) in CHCl_3 (10 mL), and a yellow suspension was formed. The mixture was refluxed for four hours. The greenish yellow mixture was left at room temperature to evaporate slowly, then a gum matter was formed, washed with ether and n-hexane several times to afford a greenish yellow ppt. then dried under vacuum. (Green solid powder, Yield: 0.044 g, 96%. M.p ($^\circ\text{C}$): 101–103).

3.3. Antibacterial Studies

The biological activity of metal-ligand complexes (**1–7**) were examined as antibacterial activity against *Staphylococcus aureus* and *Pseudomonas aeruginosa*. Additionally, the anti-fungal ability of these complexes was tested against two fungal species *Candida albicans* and *Aspergillus niger* using the disc diffusion method using the cup-plate method at 10^{-3} M concentration of its and the result was compared with Gentamicin for anti-bacterial and or Fluconazole for anti-fungi as positive drug [39]. The standard error for the experiment was $\pm 0.03\%$, and the experiments were repeated three times in the same conditions.

3.4. Computational Detail

Three different complexes were selected to study their electronic properties. At first, the structures of these complexes (**Pd(1)**, **Cd(2)**, **Cd(7)**) were optimized with B3LYP/Def2-SVP level of theory by using the Gaussian 09 program [41]. To be sure that these optimized structures are in the local minima points, the frequency analyses were performed. One negative frequency shows that the structure is in the transition state, two or more negative frequencies show that the structure is in the saddle point, and zero negative frequency shows that the structure is in the local minimum point in the potential energy. After genuine structure optimization, post-processing calculations were performed to determine the examined complexes' electrical characteristics. Frontier orbitals (**HOMO** and **LUMO**) and electrostatic potential (**ESP**) were calculated with B3LYP/Def2-TZVP level of theory. They were calculated from a formatted checkpoint file at the iso-surface density value of $0.02 \text{ e}/\text{\AA}^3$. Natural bond orbital (**NBO**) calculations such as natural charges and donor-acceptor stabilization energy were created with the NBO 6.0 program [42] at B3LYP/Def2-SVPD level. The GaussView program [43] was used to show contour plot of HOMO and LUMO.

4. Conclusions

In this study, we describe the synthesis, characterization and in-vitro antibacterial, and cytotoxic activity of novel mixed ligand Pd(II) and Cd(II) of N-picolyl-amine dithiocarbamate and phosphine ligands. The dithiocarbamate ligand coordinate as monodentate through sulfur atom. The tested compounds were examined against *Staphylococcus aureus*, *Pseudomonas aeruginosa*, *Candida albicans* and *Aspergillus niger*. Complexes **5** and **6** displayed good antibacterial activity against pathogenic bacteria and fungi species in comparison with the standard drugs and other prepared compounds. Three complexes {**Pd(1)**, **Cd(2)**, **Cd(7)**} were theoretically investigated via the DFT method. The obtained data supported the spectroscopic charts at which these complexes adopt square planar and tetrahedral geometries. However, the tetrahedral geometry was not perfect and a distorted tetrahedral structure was exhibited due to the effect of the dppe ligand.

Supplementary Materials: The following supporting information can be downloaded at: <https://www.mdpi.com/article/10.3390/molecules28052305/s1>, Figure S1: ^{31}P nmr spectrum of complex (1), Figure S2: ^{31}P nmr spectrum of complex (2), Figure S3: ^{31}P nmr spectrum of complex (3), Figure S4: ^{31}P nmr spectrum of complex (4), Figure S5: ^{31}P nmr spectrum of complex (5), Figure S6: ^{31}P nmr spectrum of complex (6), Figure S7: ^{31}P nmr spectrum of complex (7), Figure S8: ^1H nmr spectrum of complex (1), Figure S9: ^1H nmr spectrum of complex (2), Figure S10: ^1H nmr spectrum of complex (3), Figure S11: ^1H nmr spectrum of complex (5), Figure S12: ^1H nmr spectrum of complex (6) and Figure S13: ^1H nmr spectrum of complex (7).

Author Contributions: T.B.A., R.B.-A., A.S.F., H.M.J., R.B.-A., A.S.F. and A.S.M.A.-J.: conceptualization; data curation; formal analysis; methodology; visualization; writing—original draft; writing—review and editing. T.A.Y., M.M.A.-K. and S.H.K.: conceptualization; funding acquisition and writing—review and editing. All authors have read and agreed to the published version of the manuscript.

Funding: This research was supported by the Deanship of Scientific Research at Imam Mohammed Ibn Saudi Islamic University for funding this work through Research Group no. RG-21-09-80.

Institutional Review Board Statement: These studies not involving humans or animals.

Informed Consent Statement: Informed consent was obtained from all subjects involved in the study.

Data Availability Statement: In the supporting information of this article, you will find the data that supports the findings of this study.

Acknowledgments: The authors are grateful to Tikrit University for its support. In addition, the research was supported by the Deanship of Scientific Research, Imam Mohammad Ibn Saud Islamic University (IMSIU), Saudi Arabia, Grant No. RG-21-09-80.

Conflicts of Interest: The authors declare no conflict of interest.

References

- Hogarth, G. Transition metal dithiocarbamates: 1978–2003. *Prog. Inorg. Chem.* **2005**, *53*, 71–561.
- Hogarth, G. Metal-dithiocarbamate complexes: Chemistry and biological activity. *Mini-Rev. Med. Chem.* **2012**, *12*, 1202–1215. [[CrossRef](#)] [[PubMed](#)]
- Faihan, A.S.; Hatshan, M.R.; Alqahtani, A.S.; Nasr, F.A.; Al-Jibori, S.A.; Al-Janabi, A.S. New divalent metal ion complexes with 1,8-diaminonaphthalene-2-thione: Synthesis, Spectroscopic, anti-bacterial and anticancer activity studies. *J. Mol. Struct.* **2022**, *1247*, 131291. [[CrossRef](#)]
- Faihan, A.S.; Hatshan, M.R.; Kadhim, M.M.; Alqahtani, A.S.; Nasr, F.A.; Saleh, A.M.; Al-Jibori, S.A.; Al-Janabi, A.S. Promising bio-active complexes of platinum (II) and palladium (II) derived from heterocyclic thiourea: Synthesis, characterization, DFT, molecular docking, and anti-cancer studies. *J. Mol. Struct.* **2022**, *1252*, 132198. [[CrossRef](#)]
- Al-Mouqdady, O.D.; Al-Janabi, A.S.; Hatshan, M.R.; Al-Jibori, S.A.; Fiahan, A.S.; Wagner, C. Synthesis, characterization, anti-bacterial and anticancer activities of Palladium (II) mixed ligand complexes of 2-mercapto-5-methyl-1, 3, 4-thiadiazole (HmtzS) and phosphines. Crystal structure of [Pd (mtzS) 2 (dppf)]. H_2O . EtOH. *J. Mol. Struct.* **2022**, *1264*, 133219. [[CrossRef](#)]
- Faihan, A.S.; Al-Jibori, S.A.; Al-Janabi, A.S. Novel base-free dianion complexes of Pt(II) and Pd(II) derived from heterocyclic thiourea and tertiary phosphine ligands. *J. Mol. Struct.* **2022**, *1251*, 131966. [[CrossRef](#)]
- Halimehjani, A.Z.; Marjani, K.; Ashouri, A.; Amani, V. Synthesis and characterization of transition metal dithiocarbamate derivatives of 1-aminoadamantane: Crystal structure of (N-adamantyl)dithiocarbamate)nickel(II). *Inorganica Chim. Acta* **2011**, *373*, 282–285. [[CrossRef](#)]
- Kitagawa, S.; Munakata, M.; Shimono, H.; Matsuyama, S.; Masuda, H. Synthesis and crystal structure of hexanuclear copper (I) complexes of μ_3 -pyridine-2-thionate. *J. Chem. Soc. Dalton Trans.* **1990**, *7*, 2105–2109. [[CrossRef](#)]
- Onwudiwe, D.C.; Arfin, T.; Strydom, C.A.; Kriek, R.J. Synthesis, spectroscopic characterization and behavior of AC impedance spectroscopy of Cd(II) bis(N-para-methylphenyl dithiocarbamate). *Electrochimica Acta* **2013**, *104*, 19–25. [[CrossRef](#)]
- Memon, A.A.; Afzaal, M.; Malik, M.A.; Nguyen, C.Q.; O'Brien, P.; Raftery, J. The N-alkyldithiocarbamate complexes [M (S_2CNHR) $_2$](M = Cd (ii) Zn (ii); R = C_2H_5 , C_4H_9 , C_6H_{13} , $\text{C}_{12}\text{H}_{25}$); their synthesis, thermal decomposition and use to prepare of nanoparticles and nanorods of CdS. *Dalton Trans.* **2006**, *37*, 4499–4505. [[CrossRef](#)]
- Kumar, V.; Singh, V.; Gupta, A.N.; Manar, K.K.; Drew, M.G.B.; Singh, N. Influence of ligand environments on the structures and luminescence properties of homoleptic cadmium(ii) pyridyl functionalized dithiocarbamates. *Crystengcomm* **2014**, *16*, 6765–6774. [[CrossRef](#)]
- Trindade, T.; O'Brien, P. Synthesis of CdS and CdSe nanoparticles by thermolysis of diethyldithio-or diethyldiseleno-carbamates of cadmium. *J. Mater. Chem.* **1996**, *6*, 343–347. [[CrossRef](#)]

13. Tan, Y.S.; Sudlow, A.L.; Molloy, K.C.; Morishima, Y.; Fujisawa, K.; Jackson, W.J.; Henderson, W.; Halim, S.N.B.A.; Ng, S.W.; Tiekink, E.R. Supramolecular isomerism in a cadmium bis (*N*-hydroxyethyl, *N*-isopropylthiocarbamate) compound: Physicochemical characterization of ball ($n = 2$) and chain ($n = \infty$) forms of $\{Cd [S_2CN (iPr) CH_2CH_2OH]_2 \cdot solvent\}_n$. *Cryst. Growth Des.* **2013**, *13*, 3046–3056. [\[CrossRef\]](#)
14. Thirumaran, S.; Ramalingam, K.; Bocelli, G.; Righi, L. XPS, single crystal X-ray diffraction and cyclic voltammetric studies on 1,10-phenanthroline and 2,2'-bipyridine adducts of bis (piperidinecarbodithioato-*S,S'*) cadmium (II) with CdS_4N_2 environment—A stereochemical and electronic distribution investigation. *Polyhedron* **2009**, *28*, 263–268. [\[CrossRef\]](#)
15. Faraglia, G.; Fregona, D.; Sitran, S.; Giovagnini, L.; Marzano, C.; Baccichetti, F.; Casellato, U.; Graziani, R. Platinum (II) and palladium (II) complexes with dithiocarbamates and amines: Synthesis, characterization and cell assay. *J. Inorg. Biochem.* **2001**, *83*, 31–40. [\[CrossRef\]](#)
16. Faihan, A.S.; Al-Jibori, S.A.; Hatshan, M.R.; Al-Janabi, A.S. Antibacterial, spectroscopic and X-ray crystallography of newly prepared heterocyclic thiourea dianion platinum (II) complexes with tertiary phosphine ligands. *Polyhedron* **2022**, *212*, 115602. [\[CrossRef\]](#)
17. Fregona, D.; Giovagnini, L.; Ronconi, L.; Marzano, C.; Trevisan, A.; Sitran, S.; Biondi, B.; Bordin, F. Pt (II) and Pd (II) derivatives of ter-butylsarcosinedithiocarbamate: Synthesis, chemical and biological characterization and in vitro nephrotoxicity. *J. Inorg. Biochem.* **2003**, *93*, 181–189. [\[CrossRef\]](#)
18. Marzano, C.; Fregona, D.; Baccichetti, F.; Trevisan, A.; Giovagnini, L.; Bordin, F. Cytotoxicity and DNA damage induced by a new platinum(II) complex with pyridine and dithiocarbamate. *Chem. Interact.* **2002**, *140*, 215–229. [\[CrossRef\]](#)
19. Marzano, C.; Trevisan, A.; Giovagnini, L.; Fregona, D. Synthesis of a new platinum(II) complex: Anticancer activity and nephrotoxicity in vitro. *Toxicol. Vitro* **2002**, *16*, 413–419. [\[CrossRef\]](#)
20. Mansouri-Torshizi, H.; Saeidifar, M.; Divsalar, A.; Saboury, A.A. Interaction studies between a 1, 10-phenanthroline adduct of palladium (II) dithiocarbamate anti-tumor complex and calf thymus DNA. A synthesis spectral and in-vitro study. *Spectrochim. Acta Part A Mol. Biomol. Spectrosc.* **2010**, *77*, 312–318. [\[CrossRef\]](#)
21. Khan, M.S.; Hayat, M.U.; Khanam, M.; Saeed, H.; Owais, M.; Khalid, M.; Shahid, M.; Ahmad, M. Role of biologically important imidazole moiety on the antimicrobial and anticancer activity of Fe(III) and Mn(II) complexes. *J. Biomol. Struct. Dyn.* **2021**, *39*, 4037–4050. [\[CrossRef\]](#) [\[PubMed\]](#)
22. Chen, J.; Cheng, F.; Luo, D.; Huang, J.; Ouyang, J.; Nezamzadeh-Ejhi, A.; Khan, M.S.; Liu, J.-Q.; Peng, Y. Recent advances in Ti-based MOFs in biomedical applications. *Dalton Trans.* **2022**, *51*, 14817–14832. [\[CrossRef\]](#) [\[PubMed\]](#)
23. Wang, H.; Wei, J.; Jiang, H.; Zhang, Y.; Jiang, C.; Ma, X. Design, Synthesis and Pharmacological Evaluation of Three Novel Dehydroabietyl Piperazine Dithiocarbamate Ruthenium (II) Polypyridyl Complexes as Potential Antitumor Agents: DNA Damage, Cell Cycle Arrest and Apoptosis Induction. *Molecules* **2021**, *26*, 1453. [\[CrossRef\]](#) [\[PubMed\]](#)
24. Duminy, W.; Pillay, M.N.; van Zyl, W.E. Silver(I) and Gold(I) Mono-thiocarbonate Complexes: Synthesis, Structure, Luminescence. *Inorganics* **2022**, *10*, 19. [\[CrossRef\]](#)
25. Pozza, M.D.; Orvain, C.; Brustolin, L.; Pettenuzzo, N.; Nardon, C.; Gaiddon, C.; Fregona, D. Gold(III) to Ruthenium(III) Metal Exchange in Dithiocarbamate Complexes Tunes Their Biological Mode of Action for Cytotoxicity in Cancer Cells. *Molecules* **2021**, *26*, 4073. [\[CrossRef\]](#)
26. Alhoshani, A.; Sulaiman, A.; Sobeai, H.; Qamar, W.; Alotaibi, M.; Alhazzani, K.; Monim-Ul-Mehboob, M.; Ahmad, S.; Isab, A. Anticancer Activity and Apoptosis Induction of Gold(III) Complexes Containing 2,2'-Bipyridine-3,3'-dicarboxylic Acid and Dithiocarbamates. *Molecules* **2021**, *26*, 3973. [\[CrossRef\]](#)
27. Geary, W.J. The use of conductivity measurements in organic solvents for the characterization of coordination compounds. *Coord. Chem. Rev.* **1971**, *7*, 81–122. [\[CrossRef\]](#)
28. Al-Janabi, A.S.; Jerjes, H.M.; Salah, M.H. Synthesis and characterization of new metal complexes of thione and phosphines Ligands. *Tikrit J. Pure Sci.* **2018**, *22*, 53–57.
29. Al-Janabi, A.S.M.; Al-Nassiry, A.I. Synthesis, characterization and antibacterial studies of some of phenyl mercury (II) complexes of 1, 3-benzothiazole-2-thione and phosphine or amines. *Res. J. Chem. Environ.* **2020**, *24*, 90–97.
30. Al-Janabi, A.S.; Al-Soumadi, G.A.; Kheir-Allah, B.A. Preparation ligand 5-(3-chlorophenyl)-1,3,4-oxadiazole-2-thiol by new method and complexation with transition metals. *Orient. J. Chem.* **2011**, *27*, 1465.
31. Brisdon, A.; Nakamoto, K. *Infrared and Raman Spectra of Inorganic and Coordination Compounds, Part B, Applications in Coordination, Organometallic, and Bioinorganic Chemistry*, 6th ed.; Wiley: New York, NY, USA, 2010.
32. Kuchen, W.; Buchwald, H. Zur Kenntnis der Organophosphorverbindungen, II. Das Tetraphenyldiphosphin. *Eur. J. Inorg. Chem.* **1958**, *91*, 2871–2877. [\[CrossRef\]](#)
33. Witschard, G.; Griffin, C. Infrared absorption characteristics of alkyl and aryl substituted phosphonium salts. *Spectrochim. Acta* **1963**, *19*, 1905–1910. [\[CrossRef\]](#)
34. Al-Janabi, A.S.; Kadhim, M.M.; Al-Nassiry, A.I.; Yousef, T.A. Antimicrobial, computational, and molecular docking studies of Zn (II) and Pd (II) complexes derived from piperidine dithiocarbamate. *Appl. Organomet. Chem.* **2021**, *35*, e6108. [\[CrossRef\]](#)
35. Salman, M.M.; Al-Dulaimi, A.A.; Al-Janabi, A.S.; Alheety, M.A. Novel dithiocarbamate nano Zn (II), Cd (II) and Hg (II) complexes with pyrrolidinedithiocarbamate and *N,N*-diethyldithiocarbamate. *Mater. Today Proc.* **2021**, *43*, 863–868. [\[CrossRef\]](#)

36. Al-Janabi, A.S.; Al-Samrai OA, A.; Yousef, T.A. New palladium (II) complexes with 1-phenyl-1H-tetrazole-5-thiol and diphosphine. Synthesis, characterization, biological, theoretical calculations and molecular docking studies. *Appl. Organomet. Chem.* **2020**, *34*, e5967. [\[CrossRef\]](#)
37. Faihan, A.S.; Aziz, N.M.; Ashfaq, M.; Hassan, W.M.; Al-Jibori, S.A.; Al-Janabi, A.S.; Tahir, M.N.; Al-Barwari, A.S. Synthesis, characterization, and x-ray crystallography of unexpected chloro-substitution on 1-(4-chlorophenyl)-3-phenylthiourea platinum(II) complex with tertiary phosphine ligand. *J. Mol. Struct.* **2022**, *1270*, 133985. [\[CrossRef\]](#)
38. Van Beusichem, M.; Farrell, N. Activation of the trans geometry in platinum antitumor complexes. Synthesis, characterization, and biological activity of complexes with the planar ligands pyridine, *N*-methylimidazole, thiazole, and quinoline. Crystal and molecular structure of trans-dichlorobis (thiazole) platinum (II). *Inorg. Chem.* **1992**, *31*, 634–639.
39. Bauer, A.W.; Perry, D.M.; Kirby, W.M.M. Single disc antibiotic sensitivity testing of Staphylococci. *AMA Arch. Intern. Med.* **1959**, *104*, 208–216. [\[CrossRef\]](#)
40. Abdullah, T.B.; Jirjes, H.M.; Faihan, A.S.; Al-Janabi, A.S. Spectroscopic, computational, anti-bacterial studies of bivalent metal complexes of *N*-picolyl-amine dithiocarbamate. *J. Mol. Struct.* **2023**, *1276*, 134730. [\[CrossRef\]](#)
41. Frisch, M.J.; Trucks, G.W.; Schlegel, H.B.; Scuseria, G.E.; Robb, M.A.; Cheeseman, J.R.; Scalmani, G.; Barone, V.; Mennucci, B.; Petersson, G.A.; et al. *Fox Gaussian 09 Rev. E.01*; Gaussian Inc.: Wallingford, CT, USA, 2009.
42. Glendening, E.D.; Landis, C.R.; Weinhold, F. NBO 6.0: Natural bond orbital analysis program. *J. Comput. Chem.* **2013**, *34*, 1429–1437. [\[CrossRef\]](#)
43. Roy, D.; Keith, T.A.; Millam, J.M. *GaussView, Version 5.0*; Semichem Inc.: Shawnee Mission, KS, USA, 2016.

Disclaimer/Publisher's Note: The statements, opinions and data contained in all publications are solely those of the individual author(s) and contributor(s) and not of MDPI and/or the editor(s). MDPI and/or the editor(s) disclaim responsibility for any injury to people or property resulting from any ideas, methods, instructions or products referred to in the content.